JCTC Journal of Chemical Theory and Computation

ARTICLE

pubs.acs.org/JCTC

Encapsulation Influence on EPR Parameters of Spin-Labels: 2,2,6,6-Tetramethyl-4-methoxypiperidine-1-oxyl in Cucurbit[8]uril

Zilvinas Rinkevicius,*[,†,§] Bogdan Frecuș,[†] N. Arul Murugan,[†] Olav Vahtras,[†] Jacob Kongsted,[‡] and Hans Ågren[†]

[†]Department of Theoretical Chemistry & Biology, School of Biotechnology, Royal Institute of Technology, SE-106 91 Stockholm, Sweden

[‡]Department of Physics, Chemistry and Pharmacy, University of Southern Denmark, Campusvej 55, DK-5230 Odense M, Denmark

[§]Swedish e-Science Research Center (SeRC), Royal Institute of Technology, SE-100 44 Stockholm, Sweden

ABSTRACT: Encapsulation of a nitroxide spin label into a host cavity can prolong the lifetime of the spin label in biological tissues and other environments. Although such paramagnetic supramolecular complexes have been extensively studied experimentally, there is yet little understanding of the role of the encapsulation on the magnetic properties of the spin labels and their performance at the atomistic level. In this work, we approach this problem by modeling encapsulation induced changes of the magnetic properties of spin labels for a prototypical paramagnetic guest−host complex, 2,2,6,6-tetramethyl-4-methoxypiperidine-1-oxyl, enclosed in the hydrophobic cavity of cucurbit[8]uril, using state-of-the-art hybrid quantum mechanics/molecular mechanics methodology. The results allow a decomposition of the encapsulation shift of the electronic **g**-tensor and the nitrogen isotropic hyperfine coupling constant of nitroxide radical into a set of distinct contributions associated with the host cavity confinement and with changes of the local solvent environment of the spin label upon encapsulation. It is found that the hydrophobic cavity of cucurbit[8]uril only weakly influences the electronic **g**-tensor of the 2,2,6,6-tetramethyl-4-methoxypiperidine-1-oxyl but induces a significant encapsulation shift of the nitrogen hyperfine coupling constant. The latter is caused by the change of topology of the hydrogen bonding network and the nature of the hydrogen bonds around the spin label induced by the hydrophobic cavity of the inclusion host. This indirect effect is found to be more important than the direct influence of the cavity exerted on the radical. The ramification of this finding for the use of approximate methods for computing electron paramagnetic resonance spectra of spin labels and for designing optimal spin labels based on guest−host templates is discussed.

1. INTRODUCTION

Electron paramagnetic resonance (EPR) spectroscopy is a most versatile technique for studies of biomolecules in controlled environments,[1−12] like solvents or crystals. This technique has extensively been used for exploitation of structure; surface properties; and dynamics of proteins, membranes, and other biological complexes, prevalently employing nitroxides as spin labels owing to their chemical stability.[1−8,11,12] However, only a handful of such studies have yet been carried out in native biological environments,[13−18] *in vivo* or *in vitro*, due to the reduced stability of nitroxides or other spin labels in such environments.

The major chemical obstacles for *in vivo* EPR spin labeling studies are the rapid one-electron reduction of the nitroxide radical to the corresponding EPR silent hydroxylamine[19−22] as well as the two-electron cellular bioreduction which may occur following the oxidation of the stable spin label.[23] Moreover, the reduction of nitroxides in biological tissues depends on the concentration of oxygen and endogenous reducing agents, such as glutathione,[19,24] and on the spin label structure (piperidine vs pyrrolidine ring).[25]

A way to overcome these problems is to increase the steric hindrance around the spin label, thus employing a molecular complex which encapsulates the nitroxide into a protective cavity that can effectively increase the time during which the EPR signal can be detected.[20−22] However, the inclusion of the nitroxide spin label into a protective host cavity introduces the additional complexity that the spectral changes of the EPR signal caused by the host cavity, the solvent, and the target system, cannot be disentangled without microscopic knowledge of the interactions involved. This work is an attempt to resolve this matter and to advance the understanding of the mechanisms governing the changes of the EPR spin Hamiltonian parameters of spin labels under encapsulation. For this purpose, we apply state-of-the-art molecular modeling techniques comprising hybrid quantum mechanics/molecular mechanics for the evaluation of EPR spin Hamiltonian parameters,[26−29] and we study a prototypical paramagnetic guest−host system, 2,2,6,6-tetramethyl-4-methoxypiperidine-1-oxyl in cucurbit[8]uril, which has been recently extensively studied using experimental EPR methods.[20] This is part of an effort to design more reliable procedures for EPR spectra analysis, which takes into account various microscopic mechanisms responsible for spin Hamiltonian parameters, being applicable, in addition to "guest−host" complexes, to spin-labels restrained within hydrophobic cavities on protein surfaces.

2. COMPUTATIONAL DETAILS

In this work, an integrated approach[30,31] has been employed to evaluate EPR spin Hamiltonian parameters of the 2,2,6,6-tetramethyl-4-methoxypiperidine-1-oxyl (4M) radical in either

Received: November 14, 2011
Published: December 07, 2011

aqueous solution or encapsulated within the molecular cavity of cucurbit[8]uril (CB[8]) also embedded in an aqueous solution. This approach consists of two steps—classical molecular dynamics (MD) simulations of the solute in its solvent environment and subsequent hybrid quantum mechanics/molecular mechanics (QM/MM) methodology based calculations of EPR spin Hamiltonian parameters over the set of uncorrelated snapshots extracted from the MD trajectory. In the following, we will describe the technical details of both computational steps of this integrated approach, which has been used in this work to study encapsulation effects on the EPR spin Hamiltonian parameters of the 4M radical.

2.1. Classical Molecular Dynamics Simulations. In this work we carried out two separate molecular dynamics simulations at ambient temperature: one for the 4M radical in aqueous solution and a second for the 4M encapsulated in the cavity of CB[8], a guest−host complex in aqueous solution. In the first MD simulation, the 4M radical was solvated in an orthorhombic box with dimensions of approximately 69.6, 68.1, and 65.4 Å and which contained 10 192 water solvent molecules. In the second MD simulation, the solvent box dimension was approximately 76.4, 71.5, and 75.8 Å and contained 13 567 water molecules as well as the 4M@CB guest−host complex. Both simulations have been performed within the isothermal−isobaric ensemble, and the temperature and pressure have been controlled by connecting the simulation box to a thermostat and a barostat.[32−34] The MD simulations have been carried out using the AMBER molecular dynamics package.[35] Concerning the force fields used in the MD simulations, we used the TIP3P[36] force field to describe the water molecules and the GAFF[37] force field for the CB[8] molecule. The CB[8] atomic charges have been derived using the CHELPG[38] procedure at the B3LYP/6-311++G(d,p) level. In addition to this rather conventional force field choice, we have faced the challenge of selecting a suitable force field for the 4M radical, which would provide a reliable description of the structural parameters of the $R_2NO^{\bullet}$ moiety in the 4M radical. After evaluating several alternative force fields designed for description of the nitroxides and spin labels, we settled on a recently developed extension of the AMBER force field by Barone et al.[39] A time step of 1 fs has been chosen for the integration of the equation of motion. Using the above outlined setup, the MD simulations have been carried out for the free 4M radical and the 4M@CB[8] guest−host complex in aqueous solution, where the production trajectory length was set to 0.5 ns after an equilibration run of 0.5 ns. From both MD simulations, we extracted 100 snapshots, which have been taken with regular 5 ps time intervals from the production MD trajectory, for subsequent QM/MM calculations of EPR spin Hamiltonian parameters in the second step of the integrated approach for molecular properties modeling.

2.2. Hybrid QM/MM Calculations of EPR Spin-Hamiltonian Parameters. The EPR spin-Hamiltonian parameters of the 4M radical, i.e., the electronic **g**-tensor and nitrogen isotropic hyperfine coupling constant (hfcc), have in this work been computed using the hybrid density functional theory/molecular mechanics approach[28] and the hybrid density functional restricted−unrestricted theory/molecular mechanics approach,[29] respectively. In these calculations, we employed a well established setup for evaluation of both parameters, which have been extensively benchmarked in our previous works on the prototypical system, di-tert-butyl-nitroxide in aqueous solution.[28,29] Thus, according to the methodology suggested in our previous works,[28,29] we carried out electronic **g**-tensor and nitrogen isotropic hfcc calculations limiting the QM region to the 4M radical and treating the CB[8] molecule and all molecules within a 20 Å radius around the 4M radical as the MM region. The QM region has been described at the B3LYP[40−43] level using the Huz-III basis set[44,45] for electronic **g**-tensor calculations, while in the case of the nitrogen isotropic hfcc calculations we have used the more flexible core region basis set Huz-IIIsu3.[44,45] Here, we would like to point out that the selection of the B3LYP functional for our calculations is motivated by our desire to have the same level description of the 4M radical during evaluation of both spin-Hamiltonian parameters, as this allows us to compare the encapsulation effect on both spin Hamiltonian parameters more fairly. However, as we already noted in our previous works,[28,29] a more accurate description of the electronic **g**-tensor and nitrogen isotropic hfcc of the 4M radical can be obtained by using the BP86[41,46] or PBE0[47−50] functionals, respectively. After outlining the technical details of the QM region description of the hybrid QM/MM calculations, let us turn to the second important technical aspect of these calculations, namely, the description of the MM region. For the water molecules in the MM region, we used the MM-3 force field,[28] which has shown very good performance in our previous works[28,29] and is thus expected to perform well in representing the aqueous environment of both the 4M radical and the 4M@CB[8] guest−host complex. The single remaining molecule in our MM region, namely, the CB[8] host molecule, has in all calculations been described using the same level of force field as the water molecules; i.e., the force field parametrization included point charges, distributed dipoles and quadrupoles, and distributed anisotropic polarizabilities. This force field has been generated following the LoProp procedure[51] at the B3LYP/6-31+G(d) level of theory and has been evaluated for each snapshot separately, thereby including molecular distortions in the CB[8] guest. All of the above outlined calculations have been carried out using the development version of the DALTON quantum chemistry program.[52]

3. RESULTS AND DISCUSSION

EPR spin Hamiltonian parameters of nitroxide spin labels show a remarkable dependence on the geometrical structure of the $R_2NO^{\bullet}$ moiety and its immediate environment. These features have, over the years, been the subject of numerous experimental and theoretical studies,[28,29,31,53−72] and by and large, the behavior of nitroxides in protic and aprotic solvents is now quite well understood. However, guest−host complexes, in which nitroxides are included in various hollow compounds like cucurbiturils, have been less extensively investigated,[20,21,73−77] and so far no studies have addressed the changes of EPR spin Hamiltonian parameters upon encapsulation of nitroxide in host cavities at the microscopic level. In order to resolve this matter and to investigate the atomistic origin of these effects, we study a prototype guest−host system (see Figure 1) consisting of the 2,2,6,6-tetramethyl-4-methoxypiperidin-1-oxyl (4M) radical and cucurbit[8]uril (CB[8]) solvated in aqueous solution. In the following, we describe the effect of encapsulation in CB[8] on the 4M internal structural parameters and the local solvation environment of the $R_2NO^{\bullet}$ moiety. Using the results for the structural parameters of the solvated 4M@CB[8] complex, it is possible to dismantle the encapsulation induced shift of the electronic **g**-tensor and the isotropic hyperfine coupling constant (hfcc) of nitrogen into distinct contributions due to the CB[8] cavity and

the bulk water solvent and into the more indirect contributions from the interplay between solvation and encapsulation effects.

The spin Hamiltonian parameters, namely, the electronic **g**-tensor and the nitrogen isotropic hyperfine coupling constant, of nitroxides are mainly governed by the structure of two orbitals:[28,29,53,59,62] the doubly occupied *n*-type HOMO, in which the oxygen lone pair resides, and the singly occupied π-type SOMO, which holds the unpaired electron (see Figure 1). These two orbitals are localized on the $R_2NO^{\bullet}$ moiety, and the geometrical structure as well as the local solvent environment of this moiety are therefore the key factors determining the values of the spin Hamiltonian parameters. Taking this into account, the first step toward understanding the influence of encapsulation on the guest spin Hamiltonian parameters is to examine the differences of the internal 4M radical structural parameters—the NO bond distance and improper dihedral angle θ (see Figure 2 for the definition of this angle)—between the two systems: the free 4M radical and the 4M@CB[8] complex solvated in water. The results of molecular dynamic simulations indicate that the dynamics of the NO bond in terms of both bond length and out-of-plane movement are almost the same for the two systems, see Figure 2. Because of the limited encapsulation effect on the dynamics of the internal 4M radical, we can expect the changes of the spin Hamiltonian parameters induced by the host cavity to be negligible. However, differently from the internal geometrical structure of the 4M radical, the encapsulation in CB[8] has a profound effect on the topology and dynamics of the local solvation of the $R_2NO^{\bullet}$ moiety in the 4M radical, where the averaged number of hydrogen bonded water molecules to the $R_2NO^{\bullet}$ oxygen decreases from 1.8 to 1.3 going from the free 4M nitroxide to the 4M@CB[8] complex in aqueous solution. Furthermore, in addition to the conventional hydrogen bonding topology "$R_2NO^{\bullet}$ moiety···water···water" two new topologies are present in the aqueous 4M@CB[8] complex (see Figure 3): "$R_2NO^{\bullet}$ moiety···water···CB[8]", where one water hydrogen bonds to both 4M and CB[8], and "$R_2NO^{\bullet}$ moiety···water···water ···CB[8]", where two waters form a hydrogen bond bridge between 4M and CB[8]. As one can see from panels c and d in Figure 3, the encapsulation of the 4M radical in CB[8] not only reduces the average number of water molecules bound to it but also changes the distribution of these waters over the MD trajectory; fewer configurations without hydrogen bonded waters to the 4M radical appear and the number of configurations with three hydrogen bonded waters to the 4M radical decreases significantly. The hydrogen bonds formed in the two cases also show some peculiarities. In the case of the 4M radical in aqueous solution, all waters hydrogen bonded to the 4M radical follow the conventional "$R_2NO^{\bullet}$ moiety···water···water" topology. Upon encapsulation of the 4M radical in CB[8], only around 4% of the hydrogen bonded water molecules retain the same hydrogen bonding topology as in case of the free 4M radical in aqueous solution, while 96% of the hydrogen bonded waters adopt the above-mentioned

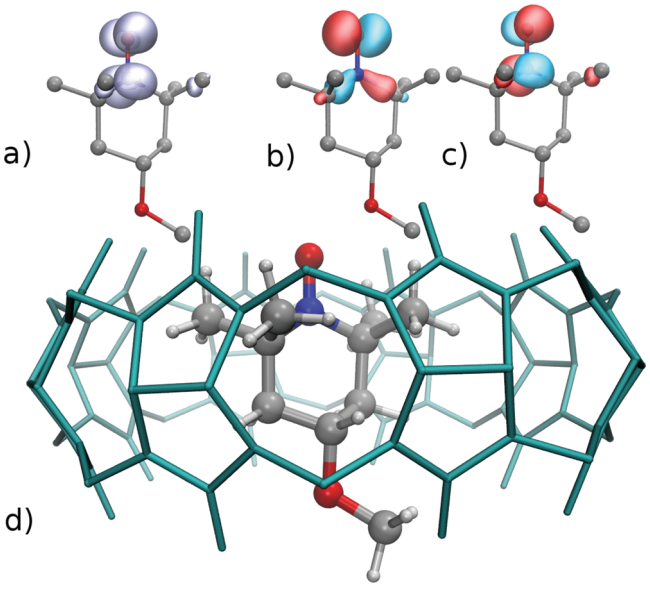

Figure 1. Graphical illustration of (a) spin density, (b) HOMO, and (c) SOMO of the 4M radical, and its inclusion complex with the CB[8] host (hydrogen atoms have been removed from CB[8] for clarity).

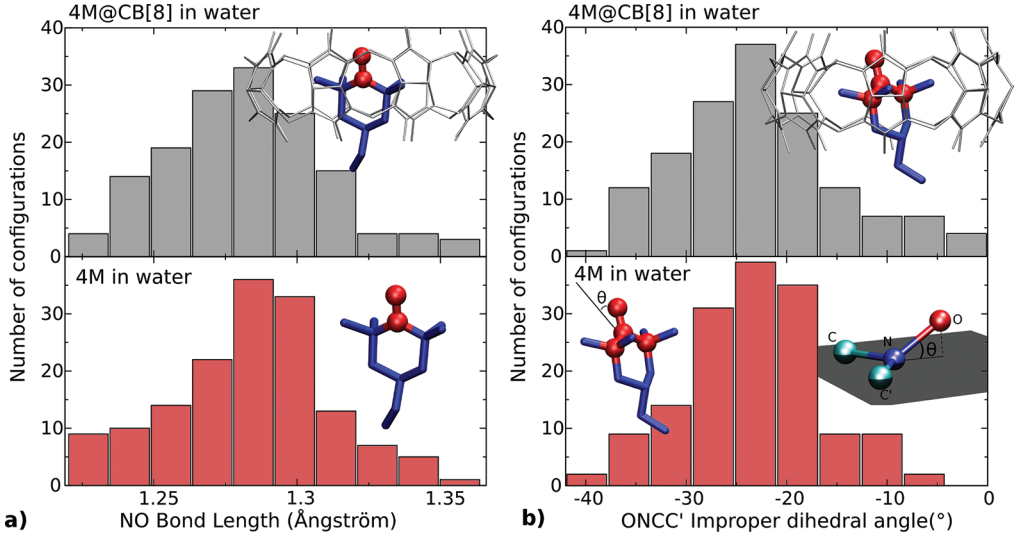

Figure 2. Internal parameters of the 4M radical and 4M@CB[8] complex in aqueous solution: (a) NO distance histograms for both MD simulations: top, 4M@CB[8] in water; bottom, −4 M in water. (b) NOCC′ improper dihedral angle histograms for both MD simulations: top, −4M@CB[8] in water; bottom, 4 M in water.

dx.doi.org/10.1021/ct200816z |*J. Chem. Theory Comput.* 2012, 8, 257–263

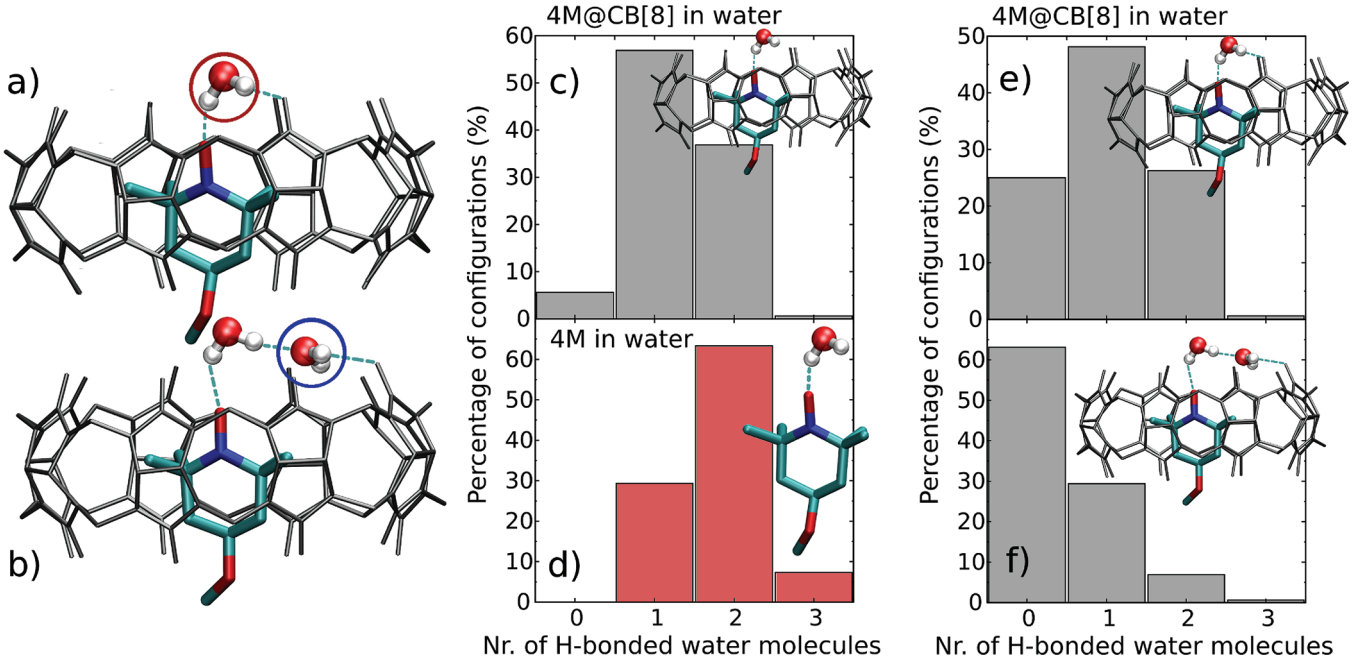

Figure 3. Graphical illustration of the supramolecular assemblies of 4M@CB[8] (hydrogen atoms have been removed for clarity) highlighting the two possible topologies that involve hydrogen-bonding solvent molecules to the guest and host systems: (a) "$R_2NO^•$ moiety···water···CB[8]" and (b) "$R_2NO^•$ moiety···water···water···CB[8]". Hydrogen bond distribution (c) 4M@CB[8] in water, (d) 4 M in water MD simulations. Distribution of new hydrogen bonding topologies in the 4M@CB[8] complex in aqueous solution: (e) "$R_2NO^•$ moiety···water···CB[8]" and (f) "$R_2NO^•$ moiety···water···water···CB[8]".

Table 1. Decomposition of the Shift in the Electronic g-Tensor and Nitrogen Isotropic hfcc in Aqueous 4M Radical Encapsulated in CB[8] Host Cavity Based on the Hybrid QM/MM Calculations[a]

origin of contribution	Δg_{iso} in ppm	a_N in Gauss
internal dynamics of $R_2NO^•$ moiety[b]	−61	−0.01
interaction with water molecules[c]	22	−0.51
interaction with CB[8][d]	12	−0.05
changes in hydrogen bond strength due to solvent and CB[8] interaction[e]	−37	0.12
total[f]	−64	−0.45
exptl.[g]	−240	−0.41

[a] EPR spin-Hamiltonian parameters computed at the Huz-III/B3LYP (**g**-tensor) and HUZ-IIIsu3/B3LYP (hfcc) levels of theory. [b] Determined as the difference between averaged vacuum values of the EPR spin-Hamiltonian parameter, which have been computed over 100 snapshots with geometries for each snapshot taken from the MD simulations of the aqueous 4M@CB[8] complex and of the aqueous radical. [c] Determined as the difference between averaged values of EPR spin-Hamiltonian parameter in aqueous solution with internal dynamics of the $R_2NO^•$ moiety subtracted. [d] Determined as the difference between averaged values of the EPR spin-Hamiltonian parameter computed for free and encapsulated 4M radical in a vacuum with snapshot geometries taken from the 4M@CB[8] complex in aqueous solution MD trajectory. [e] Determined as the difference between averaged values of the EPR spin-Hamiltonian parameter computed for the 4M radical in aqueous solution with and without a CB[8] host included in QM/MM calculations. [f] Sum of all contributions to the encapsulation shift of the EPR spin-Hamiltonian parameter. [g] Experimental EPR parameters of 4M radical in the presence of 2 mM sodium ascorbate and 3.4 mM CB[8] with the pH adjusted with LiOH, obtained by Bardelang et al.,[4] more specifically, the difference between the values reported for the aqueous solutions of the encapsulated 4M radical and free 4M radical.

two new topologies involving the CB[8] host cavity. We can expect this significant alternation of local solvation of the $R_2NO^•$ moiety upon encapsulation to be the main mechanism responsible for changes of its spin Hamiltonian parameters.

In order to shed light on the mechanism for the encapsulation induced shift of the electronic **g**-tensor and the nitrogen isotropic hfcc, we decompose the encapsulation shift into contributions of different physical origin. According to the MD simulations of the free 4M radical and the solvated 4M@CB[8] complex, we identified the following possible mechanisms for the encapsulation shift: (a) alternation of internal dynamics of the $R_2NO^•$ moiety in the 4M radical, (b) reduction of the average number of water molecules bonded to the oxygen of $R_2NO^•$, and (c) alternation of the hydrogen bond strength between $R_2NO^•$ and water molecules due to changes in the hydrogen bonding topology. In addition to these structural mechanisms, we also consider the direct effect of the CB[8] cavity on the electronic structure of the 4M radical and its EPR spin Hamiltonian parameters. The hybrid QM/MM computational results of this decomposition of the encapsulation shift of Δg_{iso} and a_N are tabulated in Table 1.

Overall, the QM/MM results qualitatively reproduce the observed encapsulation shifts of the spin Hamiltonian parameters of the 4M radical. For the electronic **g**-tensor, our calculations underestimate the experimentally observed decrease of Δg_{iso} upon the 4M radical encapsulation in CB[8]. The reason can most likely be traced to differences in conditions for the experiment and our MD simulations. In fact, by their design, the MD simulations eliminate the influence of various external factors on the 4M radical aqueous environment, which can influence experimental results and provide a more clear foundation for evaluating the encapsulation effect on the spin Hamiltonian parameters. We therefore expect our QM/MM modeling results to be representative of the influence exerted of the CB[8] cavity on the 4M radical electronic structure and its magnetic properties in aqueous solution.

The four above identified mechanisms for the encapsulation shift of Δg_{iso} are evidently of different importance. According to the results in Table 1, the change of the internal 4M radical dynamics upon encapsulation in the CB[8] cavity is responsible for the decrease of Δg_{iso} by 61 ppm and is apparently the largest contribution to the encapsulation shift of Δg_{iso}. This is a rather unexpected result, since the MD simulations indicate that the internal parameters of the $R_2NO^{\bullet}$ moiety as well as its dynamics are only minorly altered upon encapsulation in the CB[8] cavity. Out of the remaining mechanisms, the smallest contribution arises from the direct influence of the CB[8] cavity on the electronic structure of the 4M radical, which is approximately 5 times smaller than the previously discussed contribution. Furthermore, it acts in the opposite way, i.e. induces an increase of Δg_{iso} upon encapsulation (see Table 1 for details). The last two mechanisms responsible for the encapsulation shift of Δg_{iso} are related to changes of the aqueous environment of the 4M radical going from its free to its guest−host complex form. The "interaction with water molecules" mechanism includes contributions from alternation of the aqueous environment structure (waters hydrogen bonded to the 4M radical as well as waters in the bulk of the aqueous solution) upon encapsulation, which increases Δg_{iso}, as can be seen from Table 1. This is caused by the number of hydrogen bonded waters to the $R_2NO^{\bullet}$ moiety in the aqueous 4M@CB[8] complex, which in turn leads to a smaller blue shift of the $n \rightarrow \pi$ excitation (see Figure 1) and consequently to a larger Δg_{iso} of the encapsulated 4M radical compared to its free form in aqueous solution. The final mechanism of the four is the change of the hydrogen bond strength between oxygen of the $R_2NO^{\bullet}$ moiety and the water molecules, induced by the interaction of the water molecules with the CB[8] cavity. As we already established, most of the hydrogen bonds between the 4M radical and the waters in the 4M@CB[8] complex undergo an alternation of their topology, and we can thus expect this mechanism to give a significant contribution to the encapsulation shift of Δg_{iso}. The QM/MM results in Table 1 verify this assumption and show that the alternation of hydrogen bond strengths due to the water interaction with CB[8] leads to almost a doubling of the encapsulation shift of Δg_{iso} compared to the one induced by the reduction of the averaged number of hydrogen bonded waters to the 4M radical upon encapsulation. Furthermore, these two encapsulation shifts of Δg_{iso} have opposite sign, and thus their overall relative importance for the total encapsulation shift of Δg_{iso} is diminished.

Taking into account the size of the four individual contributions to the encapsulation shift of Δg_{iso}, we can establish their decreasing order of importance: "alternation of the internal dynamics of the 4M radical upon encapsulation" > "reduction of the averaged number of hydrogen bonded waters to the $R_2NO^{\bullet}$ moiety open encapsulation" + "change of the hydrogen bond nature and topology upon encapsulation" > "direct influence of the CB[8] cavity on the electronic structure of the 4M radical upon encapsulation". We conclude that the encapsulation induced shift of the **g**-tensor is rather small (−64 ppm, see Table 1) and is significantly smaller than the shift induced by solvation of the 4M radical in water as shown by the data in Table 2. Therefore, the encapsulation of the 4M radical in the CB[8] cavity in aqueous solution only slightly affects the electronic **g**-tensor of the radical, indicating that it can be disregarded in practical analysis of EPR spectra of guest−host systems of such a kind and probably also for spin-labels residing in hydrophobic cavities of proteins. Thus, the QM/MM modeling of the 4M radical **g**-tensors provides for the first time theoretical support to the common assumption in empirical models that the electronic **g**-tensor of the spin label remains unchanged upon encapsulation.

Table 2. Electronic g-Tensor and Nitrogen Isotropic Hyperfine Coupling Constants of Free 4M Radical in Water and in 4M Radical in 4M@CB[8] Complex in Water[a]

	Δg_{iso} in ppm	a_N in G
4M (vacuum)[b]	4063	14.85
4M (water)[b]	3705	17.00
4M (water) Exp.[c]	4201	17.04
4M (vacuum)[d]	4003	14.84
4M@CB[8] (water)[d]	3641	16.55
4M@CB[8] (water) exptl.[c]	3961	16.63

[a] EPR spin-Hamiltonian parameters computed at the Huz-III/B3LYP (**g**-tensor) and HUZ-IIIsu3/B3LYP (hfcc) levels of theory. [b] Structural data taken from aqueous 4M radical MD simulation. [c] Experimental data taken from the Supporting Information of ref 20. [d] Structural data taken from the aqueous 4M radical encapsulated in CB[8] MD simulation.

For the second important spin Hamiltonian parameter—the nitrogen isotropic hyperfine coupling constant a_N—we find, in agreement with previous studies of nitroxides, that the local solvent environment effect on the 4M radical is larger than that for the electronic **g**-tensor. The QM/MM results tabulated in Table 1 indicate that the encapsulation of the 4M radical in the CB[8] cavity reduces the nitrogen isotropic hfcc by the significant amount of 0.45 G. Comparing theoretical results and experimental data, the former overestimate the encapsulation shift of a_N, probably for the same reasons as in the case of the electronic **g**-tensor, i.e., a mismatch between environmental conditions for the MD simulations and the ones encountered in the real experiments. Following a similar procedure as for Δg_{iso}, we decomposed the encapsulation shift of a_N into four contributions. The first most striking difference between the electronic **g**-tensor and the nitrogen isotropic hfcc is the small contribution to the latter from the changes in internal structure and dynamics of the 4M radical, while the opposite is found in the former case. This is in line with our expectations based on the analysis of MD results, which show that the $R_2NO^{\bullet}$ moiety changes only slightly going from free 4M radical to its encapsulated form in the aqueous environment. The reason can be traced to the electron spin density, which defines the value of a_N and which is solely localized on the $R_2NO^{\bullet}$ moiety (see Figure 1). The negligible geometry change in this moiety naturally translates into

a small encapsulation shift induced via this mechanism. Concerning the direct influence of the CB[8] cavity on the 4M electronic structure, our results for the two spin Hamiltonian parameters agree well, indicating a negligible size of this contribution in both cases. The two remaining contributions to the encapsulation shift of the nitrogen isotropic hfcc are associated with changes of the aqueous environment of the 4M radical and play, as we expect, a most important role. Among these two contributions, the large change of a_N is caused by the decrease of the averaged number of water molecules bonded to the $R_2NO^{\bullet}$ moiety, while the effect of new hydrogen bonding topologies on the encapsulation shift is less pronounced, being almost 5 times smaller. Taking these results into account, we can establish the following order of the contributions to the encapsulation shift of a_N in decreasing importance: "reduction of the averaged number of hydrogen bonded waters to the $R_2NO^{\bullet}$ moiety open encapsulation" > "change of the hydrogen bond topology upon encapsulation" > "direct influence of the CB[8] cavity on the electronic structure of the 4M radical upon encapsulation" > "alternation of the internal dynamics of the 4M radical upon encapsulation". This order of the contributions is in good agreement with the one predicted on the basis of our analysis of the MD simulations and indicates that the rather unexpected behavior of the encapsulation shift of the electronic **g**-tensor should be qualified by the overall small size of the contributions making it up. In total, according to results presented in Table 2, the solvent shift of a_N is 2.14 G going from a vacuum to aqueous solution, and the encapsulation shift, being 0.45 G, thus constitutes almost 25% of the solvent shift and cannot be neglected in the analysis of experimental EPR spectra. We conclude that encapsulation produces a significant effect on this spin Hamiltonian parameter, something that can be expected to be encountered in other similar "guest−host" complexes as well as in the case of spin-labels residing in hydrophobic cavities of proteins.

4. CONCLUSIONS

In the present work, we have given a theoretical perspective on the effect of encapsulation on the magnetic properties of spin labels encased in hydrophobic host cavities consisting of a protective shell molecule. We approached this problem by employing state-of-the-art hybrid quantum mechanics/molecular mechanics, which allow for a consistent description of spin labels in different environments. We studied the encapsulation effect of the spin label electronic **g**-tensor and the nitrogen isotropic hyperfine coupling constant in a prototypical guest−host system, consisting of 2,2,6,6-tetramethyl-4-methoxypiperidine-1-oxyl and cucurbit[8]uril, in aqueous solution. From our modeling results, several conclusions could be drawn on the physical origin of the EPR parameters of the spin labels and their dependence on encapsulation and solvation. It is shown that the hydrophobic cavity of CB[8] and other similar hosts, like cyclodextrines, only weakly influences the electronic **g**-tensor of the nitroxide but induces a noticeable encapsulation shift of the nitrogen hyperfine coupling constant. This finding provides for the first time theoretical support for the common assumption used in most empirical models that the electronic **g**-tensor of spin-labels remains unchanged upon encapsulation. However, the same assumption does not hold for the nitrogen isotropic hyperfine coupling constants, which experience significant encapsulation shifts.

The main difference between the spectroscopic properties obtained for the nitroxides in guest−host complexes and for the nitroxides in solution is attributed to the steric hindrance of the nitroxides into the hydrophobic cavity, which affects the local hydrogen bonding of the solvent molecules. Thus, upon encapsulation, fewer hydrogen bonds between the spin label and the solvent molecules are formed, thereby decreasing the magnitude of the **g**-tensor shift as well as the hfcc shift. This indirect effect is found to be significantly more important than the direct interaction with the cavity host. Thus, a future strategy to exploit spin labels to study structure; surface properties; and dynamics of proteins, membranes, and other biological complexes in their native environment is to design soluble spin labels containing guest−host complexes with cavities that strike the balance between the protective effect of the cavity, which increases the lifetime of the spin label, and the posing of a minimal effect on the hydrogen bonded water molecules to the $R_2NO^{\bullet}$ moiety of the spin label. This condition must be met in order to avoid explicit consideration of the encapsulation effect for the EPR data analysis, something that can significantly reduce the information content that can be extracted.

AUTHOR INFORMATION

Corresponding Author

*E-mail: rinkevic@theochem.kth.se.

Notes

The authors declare no competing financial interest.

ACKNOWLEDGMENT

This work has been partially funded by the EU Commission (contract INFSO-RI-261523) under the ScalaLife collaboration and has been supported by a grant from the Swedish National Infrastructure Committee (SNIC) for the project "Multiphysics Modeling of Molecular Materials", SNIC 022/09-25. J.K. thanks The Danish Councils for Independent Research (STENO and Sapere Aude programmes), the Lundbeck Foundation, and the Villum foundation for financial support.

REFERENCES

(1) Klare, J.; Steinhoff, H.-J. *Photosynth. Res.* **2009**, *102*, 377–390.
(2) Subczynski, W. K.; Widomska, J.; Feix, J. B. *Free Radical Biol. Med.* **2009**, *46*, 707–718.
(3) Margittai, M.; Langen, R. *Q. Rev. Biophys.* **2008**, *41*, 265–297.
(4) Schiemann, O.; Prisner, T. F. *Q. Rev. Biophys.* **2007**, *40*, 1–53.
(5) Bennati, M.; Prisner, T. F. *Rep. Prog. Phys.* **2005**, *68*, 411–448.
(6) Mobius, K.; Savitsky, A.; Schnegg, A.; Plato, M.; Fuchs, M. *Phys. Chem. Chem. Phys.* **2005**, *7*, 19–42.
(7) Subczynski, W. K.; Kusumi, A. *Biochim. Biophys. Acta* **2003**, *1610*, 231–243.
(8) Prisner, T.; Rohrer, M.; MacMillan, F. *Annu. Rev. Phys. Chem.* **2001**, *52*, 279–313.
(9) Borbat, P. P.; Costa-Filho, A. J.; Earle, K. A.; Moscicki, J. K.; Freed, J. H. *Science* **2001**, *291*, 266–269.
(10) Deligiannakis, Y.; Louloudi, M.; Hadjiliadis, N. *Coord. Chem. Rev.* **2000**, *204*, 1–112.
(11) Hubbell, W. L.; Cafiso, D. S.; Altenbach, C. *Nat. Struct. Biol.* **2000**, *7*, 735–739.
(12) Hubbell, W. L.; Gross, A.; Langen, R.; Lietzow, M. A. *Curr. Opin. Struct. Biol.* **1998**, *8*, 649–656.
(13) Berliner, L. *Eur. Biophys. J.* **2010**, *39*, 579–588.
(14) Abramović, Z.; Brgles, M.; Habjanec, L.; Tomašić, J.; Šentjurc, M.; Frkanec, R. *Int. J. Biol. Macromol.* **2010**, *47*, 396–401.

(15) Plonka, P. M. *Exp. Dermatol.* **2009**, *18*, 472–484.
(16) Burks, S. R.; Barth, E. D.; Halpern, H. J.; Rosen, G. M.; Kao, J. P. *Biochim. Biophys. Acta* **2009**, *1788*, 2301–2308.
(17) Okazaki, S.; Mannan, M. A.; Sawai, K.; Masumizu, T.; Miura, Y.; Takeshita, K. *Free Radical Res.* **2007**, *41*, 1069–1077.
(18) Matsumoto, K.; Yahiro, T.; Yamada, K.; Utsumi, H. *Magn. Reson. Med.* **2005**, *53*, 1158–1165.
(19) Bobko, A. A.; Kirilyuk, I. A.; Grigor'ev, I. A.; Zweier, J. L.; Khramtsov, V. V. *Free Radical Biol. Med.* **2007**, *42*, 404–412.
(20) Bardelang, D.; Banaszak, K.; Karoui, H.; Rockenbauer, A.; Waite, M.; Udachin, K.; Ripmeester, J. A.; Ratcliffe, C. I.; Ouari, O.; Tordo, P. *J. Am. Chem. Soc.* **2009**, *131*, 5402–5404.
(21) Kirilyuk, I.; Polovyanenko, D.; Semenov, S.; Grigor'ev, I.; Gerasko, O.; Fedin, V.; E., B. *J. Phys. Chem. B* **2010**, *114*, 1719–1728.
(22) Kirilyuk, I. A.; Bobko, A. A.; Grigor'ev, I. A.; Khramtsov, V. V. *Org. Biomol. Chem.* **2004**, *2*, 1025–1030.
(23) Krishna, M. C.; Grahame, D. A.; Samuni, A.; Mitchell, J. B.; Russo, A. *Proc. Natl. Acad. Sci. U.S.A.* **1992**, *89*, 5537–5541.
(24) Kuppusamy, P.; Li, H.; Ilangovan, G.; Cardounel, A. J.; Zweier, J. L.; Yamada, K.; Krishna, M. C.; Mitchell, J. B. *Cancer Res.* **2002**, *62*, 307–312.
(25) Swartz, H. M.; Sentjurc, M., II. *Biochim. Biophys. Acta* **1986**, *888*, 82–90.
(26) Olsen, J. M.; Aidas, K.; Kongsted, J. *J. Chem. Theory Comput.* **2010**, *6*, 3721–3734.
(27) Olsen, J. M. H.; Kongsted, J.; Sabin, J. R.; Brändas, E. Chapter 3 - *Molecular Properties through Polarizable Embedding*; Academic Press: New York, 2011; Vol. 61, pp 107−143.
(28) Rinkevicius, Z.; Murugan, N. A.; Kongsted, J.; Aidas, K.; Steindal, A. H.; Ågren, H. *J. Phys. Chem. B* **2011**, *115*, 4350–4358.
(29) Rinkevicius, Z.; Murugan, N. A.; Kongsted, J.; Frecus, B.; Steindal, A. H.; Ågren, H. *J. Chem. Theory Comput.* **2011**, *7*, 3261–3271.
(30) Crescenzi, O.; Pavone, M.; De Angelis, F.; Barone, V. *J. Phys. Chem. B* **2004**, *109*, 445–453.
(31) Barone, V.; Cimino, P.; Pedone, A. *Magn. Reson. Chem.* **2010**, *48*, S11–S22.
(32) Nose, S. *Mol. Phys.* **1984**, *52*, 255–268.
(33) Hoover, W. G. *Phys. Rev. A* **1986**, *34*, 2499–2500.
(34) Parrinello, M.; Rahman, A. *Phys. Rev. Lett.* **1980**, *45*, 1196–1199.
(35) Case, D. *Amber 8*; University of California: San Francisco, CA, 2004.
(36) Jorgensen, W. L.; Madura, J. D. *J. Am. Chem. Soc.* **1983**, *105*, 1407–1413.
(37) Wang, J.; Wolf, R.; Caldwell, J.; Kollman, P.; Case, D. *J. Comput. Chem.* **2004**, *34*, 1157–1174.
(38) Breneman, C.; Wiberg, K. *J. Comput. Chem.* **1990**, *11*, 361–373.
(39) Stendardo, E.; Pedone, A.; Cimino, P.; Menziani, M.; Crescenzi, O.; Barone, V. *Phys. Chem. Chem. Phys.* **2010**, *12*, 11697–11709.
(40) Becke, A. D. *J. Chem. Phys.* **1993**, *98*, 5648–5652.
(41) Becke, A. D. *Phys. Rev. A* **1988**, *38*, 3098–3100.
(42) Lee, C.; Yang, W.; Parr, R. G. *Phys. Rev. B* **1988**, *37*, 785–789.
(43) Vosko, S. H.; Wilk, L.; Nusair, M. *Can. J. Phys.* **1980**, *58*, 1200–1211.
(44) Wullen, C. *Die Berechnung magnetischer Eigenschaften unter Berücksichtigung der Ele tronkorrelation: Die Multikonfigurations-Verallgemeinerung der IGLO-Methode*. PhD thesis, Ruhr-Universität, Bochum, Germany, 1992.
(45) Lantto, P.; Vaara, J.; Helgaker, T. *J. Chem. Phys.* **2002**, *117*, 5998–6009.
(46) Perdew, J. P. *Phys. Rev. B* **1986**, *33*, 8822–8824.
(47) Perdew, J. P.; Ernzerhof, M.; Burke, K. *J. Chem. Phys.* **1996**, *105*, 9982–9985.
(48) Perdew, J. P.; Burke, K.; Ernzerhof, M. *Phys. Rev. Lett.* **1996**, *77*, 3865–3868.
(49) Ernzerhof, M.; Scuseria, G. E. *J. Chem. Phys.* **1999**, *110*, 5029–5036.
(50) Adamo, C.; Barone, V. *J. Chem. Phys.* **1999**, *110*, 6158–6170.
(51) Gagliardi, L.; Lindh, R.; Karlstrom, G. *J. Chem. Phys.* **2004**, *121*, 4494–4500.
(52) DALTON. www.daltonprogram.org (accessed Dec. 2011).
(53) Kawamura, T.; Matsunami, T.; Yonezawa, T. *Bull. Chem. Soc. Jpn.* **1967**, *40*, 1111–1115.
(54) Ramachandran, C.; Pyter, R. A.; Mukerjee, P. *J. Phys. Chem.* **1982**, *86*, 3198–3205.
(55) Voinov, M. A.; Ruuge, A.; Reznikov, V. A.; Grigor'ev, I. A.; Smirnov, A. I. *Biochemistry* **2008**, *47*, 5626–5637.
(56) Owenius, R.; Engström, M.; Lindgren, M.; Huber, M. *J. Phys. Chem. A* **2001**, *105*, 10967–10977.
(57) Engström, M.; Vaara, J.; Schimmelpfennig, B.; Ågren, H. *J. Phys. Chem. B* **2002**, *106*, 12354–12360.
(58) D'Amore, M.; Improta, R.; Barone, V. *J. Phys. Chem. A* **2003**, *107*, 6264–6269.
(59) Rinkevicius, Z.; Telyatnyk, L.; Vahtras, O.; Ruud, K. *J. Chem. Phys.* **2004**, *121*, 5051–5060.
(60) Improta, R.; Barone, V. *Chem. Rev.* **2004**, *104*, 1231–1254.
(61) Neugebauer, J.; Louwerse, M. J.; Belanzoni, P.; Wesolowski, T. A.; Baerends, E. J. *J. Chem. Phys.* **2005**, *123*, 114101.
(62) Sinnecker, S.; Rajendran, A.; Klamt, A.; Diedenhofen, M.; Neese, F. *J. Phys. Chem. A* **2006**, *110*, 2235–2245.
(63) Pavone, M.; Cimino, P.; De Angelis, F.; Barone, V. *J. Am. Chem. Soc.* **2006**, *128*, 4338–4347.
(64) Barone, V.; Brustolon, M.; Cimino, P.; Polimeno, A.; Zerbetto, M.; Zoleo, A. *J. Am. Chem. Soc.* **2006**, *128*, 15865–15873.
(65) Carlotto, S.; Cimino, P.; Zerbetto, M.; Franco, L.; Corvaja, C.; Crisma, M.; Formaggio, F.; Toniolo, C.; Polimeno, A.; Barone, V. *J. Am. Chem. Soc.* **2007**, *129*, 11248–11258.
(66) Pavone, M.; Cimino, P.; Crescenzi, O.; Sillanpää, A.; Barone, V. *J. Phys. Chem. B* **2007**, *111*, 8928–8939.
(67) Houriez, C.; Ferré, N.; Masella, M.; Siri, D. *J. Chem. Phys.* **2008**, *128*, 244504.
(68) Houriez, C.; Ferré, N.; Siri, D.; Masella, M. *J. Phys. Chem. B* **2009**, *113*, 15047–15056.
(69) Houriez, C.; Ferré, N.; Masella, M.; Siri, D. *THEOCHEM* **2009**, *898*, 49–55.
(70) Pavone, M.; Biczysko, M.; Rega, N.; Barone, V. *J. Phys. Chem. B* **2010**, *114*, 11509–11514.
(71) Hermosilla, L.; García de la Vega, J. M.; Sieiro, C.; Calle, P. *J. Chem. Theory Comput.* **2011**, *7*, 169–179.
(72) Ikryannikova, L. N.; Ustynyuk, L. Y.; Tikhonov, A. N. *Magn. Reson. Chem.* **2010**, *48*, 337–349.
(73) Jayaraj, N.; Porel, M.; Ottaviani, F. M.; Maddipatla, M. V.; Modelli, A.; Da Silva, J. P.; Bhogala, B. R.; Captain, B.; Jockusch, S.; Turro, N. J.; Ramamurthy, V. *Langmuir* **2009**, *25*, 13820–13832.
(74) Mezzina, E.; Cruciani, F.; Pedulli, G.; Lucarini, M. *Chem.—Eur. J.* **2007**, *13*, 7223–7233.
(75) Mileo, E.; Mezzina, E.; Grepioni, F.; Pedulli, G. F.; Lucarini, M. *Chem.—Eur. J.* **2009**, *15*, 7859–7862.
(76) Jockusch, S.; Zeika, O.; Jayaraj, N.; Ramamurthy, V.; Turro, N. J. *J. Phys. Chem. Lett.* **2010**, *1*, 2628–2632.
(77) Mileo, E.; Yi, S.; Bhattacharya, P.; Kaifer, A. *Angew. Chem., Int. Ed.* **2009**, *48*, 5337–5340.